

# Transmission-line networks cloaking objects from electromagnetic fields

Pekka Alitalo<sup>1</sup>, Olli Luukkonen<sup>1</sup>, Liisi Jylhä<sup>2</sup>, Jukka Venermo<sup>2</sup>, Sergei Tretyakov<sup>1</sup>

<sup>1</sup>*Radio Laboratory / SMARAD Center of Excellence,  
TKK Helsinki University of Technology,  
P.O. Box 3000, FI-02015 TKK, Finland*

<sup>2</sup>*Electromagnetics Laboratory, TKK Helsinki University of Technology, Finland*

## Abstract

We consider a novel method of cloaking objects from the surrounding electromagnetic fields in the microwave region. The method is based on transmission-line networks that simulate the wave propagation in the medium surrounding the cloaked object. The electromagnetic fields from the surrounding medium are coupled into the transmission-line network that guides the waves through the cloak thus leaving the cloaked object undetected. The cloaked object can be an array or interconnected mesh of small inclusions that fit inside the transmission-line network.

## I. INTRODUCTION

Recently the subject of cloaking objects from electromagnetic fields has aroused a lot of interest. Devices capable of cloaking an object from the surrounding electromagnetic fields have been recently suggested [1, 2, 3, 4]. A realization of an electromagnetic cloak, operating in the microwave regime has been manufactured and measured [5]. The operation of the cloaks discussed in [1, 2, 3, 4, 5] is based on mapping of the electromagnetic fields in such a way that the waves that come in contact with the cloak, are guided *around* the object which is placed inside the cylindrical or spherical cloak. The main drawback of the designs presented in [1, 2, 3, 4, 5] is that these systems are capable of cloaking from time-harmonic fields only. This is because the waves that go around the cloaked object need to go as fast as the wave propagating in free space on a straight line. No signal can therefore be fully cloaked because the group velocity in the (passive) cloak can never exceed the speed of light. Also another approach to cloak design, based on hard surfaces, was proposed in [6]. This approach has the drawback of strong anisotropy, since the operation of the structure depends strongly on the incidence angle of the illuminating wave.

In this paper we present a novel idea for realization of an electromagnetic cloak operating in the microwave region. The operation of the cloak is based on transmission-line (TL) networks which can be unloaded or periodically loaded by lumped elements, such as capacitors and inductors [7, 8]. The cloak itself is composed of these networks and the wave coming from the surrounding medium travels through the cloak inside the transmission-line network (no field mapping is needed). The space between the neighboring transmission lines of the network is left undetected, i.e., cloaked from the electromagnetic fields.

The evident drawback of this approach is that a large bulky object cannot be cloaked due to the periodicity of the transmission-line network. On the other hand, the cloaked object does not have to be composed of tiny pieces that are not in contact with each other, but it can be a three-dimensional mesh of metal or any material. Also, it is clear that because no field mapping and no exotic material parameters are required, the cloak design and manufacturing are fairly straightforward. For simplification we consider only a two-dimensional cylindrical cloak here (infinite in the axial direction). However, the same approach can be easily realized also in three dimensions and for arbitrary shapes, while preserving full isotropy of (voltage and current) waves traveling inside the network, see e.g. [9].

## II. OPERATION OF THE CLOAK

The cloak that we study in this paper is a two-dimensional simplification of an isotropic three-dimensional cloak, as was also the design realized in [5]. Because the cloak is based on a transmission-line network, it is fairly easy to extend to three dimensions as well: recently the interest in obtaining isotropic TL-based metamaterials for superlensing applications has resulted in the development of different loaded and unloaded three-dimensional isotropic transmission-line networks [9, 10, 11].

The cloak design and principle of operation are illustrated in Fig. 1, where a cylindrically shaped cloak (infinite in the  $z$ -direction) is placed in free space. The operation and optimization of the properties of the cloak naturally depends on the background medium. In this paper we consider cloaking in free space (as in [1, 2, 3, 4, 5, 6]). The principle of operation is as following: The incident electromagnetic wave in free space arrives to the surface of the cloak, couples into the transmission-line network, and is guided *through* the cloak that encompasses the object(s) that we want to be hidden. The cloaked object can be a collection of small objects, or it can be a mesh of interconnected objects. The only limitation on the size of the hidden object is that it must fit inside the network.

There are two preconditions that have to be met in order that the cloak would operate ideally. Firstly, the wave propagation in the transmission-line network should mimic the wave propagation in free space, i.e., the wave propagation should be isotropic and lie on

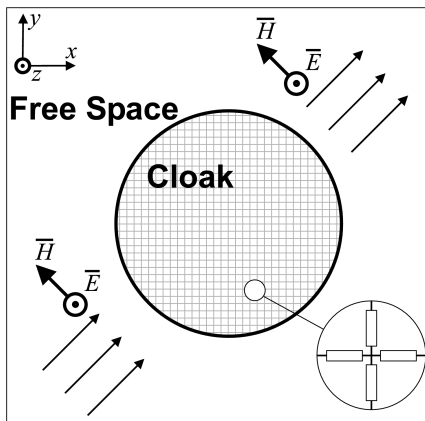


FIG. 1: A two-dimensional cylindrical electromagnetic cloak. The cloak operation does not depend on the incidence angle of the illuminating electromagnetic wave, as long as the network period is small enough with respect to the wavelength.

the same dispersion curve as that in free space. If this precondition is not satisfied, the cloak will scatter. Secondly, the transmission-line network should be impedance-matched to free space in order to prevent reflections from the cloak. The impedance matching includes also the requirement that there exists a transition layer around the cloak which couples the waves propagating in free space into the network. This transition layer can be realized e.g. with an antenna array.

### III. DISPERSION AND IMPEDANCE IN LOADED AND UNLOADED TRANSMISSION-LINE NETWORKS

To study the propagation inside a transmission-line network, we derive the dispersion equations for a loaded two-dimensional transmission-line network, where the loads are defined only as series impedance  $Z$  and shunt admittance  $Y$ . Here we can use the same derivation procedure as in [9] for a three-dimensional loaded transmission-line network, where the loads were defined as  $Z = 1/(j\omega C)$  and  $Y = 1/(j\omega L)$ ,  $C$  and  $L$  being the capacitance and inductance of the lumped loads. The dispersion equation for a 3D-case with arbitrary loads  $Z$  and  $Y$  reads:

$$\cos(k_x d) + \cos(k_y d) + \cos(k_z d) = \frac{Y}{2S} - 3\frac{K}{S}, \quad (1)$$

and for the 2D-case:

$$\cos(k_x d) + \cos(k_y d) = \frac{Y}{2S} - 2\frac{K}{S}, \text{ where} \quad (2)$$

$$S = \frac{Z}{(ZA_{TL} + B_{TL})(ZD_{TL} + B_{TL}) - B_{TL}^2}, \quad (3)$$

$$K = \frac{Z(A_{TL}D_{TL} - B_{TL}C_{TL})(ZA_{TL} + B_{TL})}{[(ZA_{TL} + B_{TL})(ZD_{TL} + B_{TL}) - B_{TL}^2]B_{TL}} - \frac{A_{TL}}{B_{TL}}, \quad (4)$$

$$\begin{bmatrix} A_{TL} & B_{TL} \\ C_{TL} & D_{TL} \end{bmatrix} = \begin{bmatrix} \cos(k_{TL}d/2) & jZ_{TL} \sin(k_{TL}d/2) \\ jZ_{TL}^{-1} \sin(k_{TL}d/2) & \cos(k_{TL}d/2) \end{bmatrix}, \quad (5)$$

$k_i$  is the wavenumber in the network along axis  $i$ ,  $d$  is the period and  $k_{TL}$  and  $Z_{TL}$  are the wavenumber and impedance of the transmission lines, respectively. The wavenumber in the network is  $k = \sqrt{k_x^2 + k_y^2 + k_z^2}$ .

Obviously the simplest transmission-line network is an unloaded one. The dispersion equation for an unloaded network is obtained by using (2) and choosing  $Z = 0$  and  $Y = 0$ . We have chosen the dimensions and impedance values for the unloaded network in such a way that the impedance of the network is approximately equal to the free space impedance, i.e.,  $377 \Omega$ , at frequency  $f = 1$  GHz. See Table I for the parameters of the unloaded network ( $k_0$  is the free space wavenumber) and Fig. 2 for the plotted dispersion curves for axial and diagonal propagation. From Fig. 2 it is clear that the phase velocity  $v_{\text{phase}} = \omega/k$  in the network slightly differs from that in free space (light line) for  $k > 0$ .

A capacitively loaded transmission-line network can be designed in such a way that its phase velocity equals that in free space for a given frequency point. This can be done by choosing  $Z = 1/(j\omega C)$  and  $Y = 0$  in (2). We have designed this network in such a way that the propagation in the network and the impedance of the network are matched with free space at  $f = 1$  GHz. See Table I for the parameters of this capacitively loaded network and Fig. 2 for the plotted dispersion curves.

TABLE I: Transmission-line network parameters.

-	$d$	$k_{\text{TL}}$	$Z_{\text{TL}}$	$C$
Loaded TL	8 mm	$k_0$	$755 \Omega$	2.5 pF
Unloaded TL	8 mm	$k_0$	$535 \Omega$	-

The required isotropy of the networks is achieved if the period is small compared to the wavelength. From Fig. 2 we can conclude that for the presented designs the isotropy is achieved for both networks approximately below 3 GHz. In Fig. 3 the impedances of the two studied networks are calculated using the equations for the network impedances derived in [9].

From the above discussion, we can conclude that the both types of networks have certain benefits and drawbacks. Although the phase velocity can be ideal for the loaded network, the group velocity is smaller than the speed of light. This means that the loaded network has the same restriction of cloaking from time-harmonic fields only, as the designs in [1, 2, 3, 4, 5]. On the other hand, in the unloaded network, the phase velocity equals the group velocity. This enables cloaking from signals. However, the phase (and group) velocities are not ideal since they do not equal to those in free space. In the rest of this paper, we will concentrate on studying the unloaded network, due to the possibility of signal operation and inherently

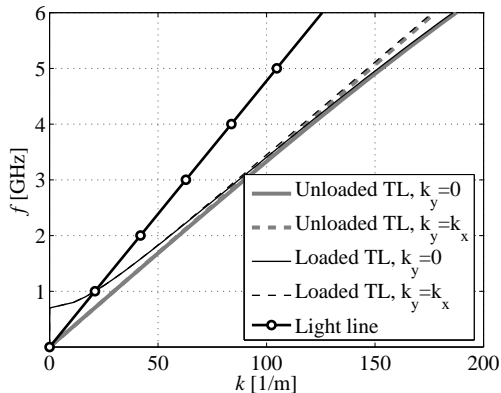


FIG. 2: Dispersion in unloaded and loaded transmission-line networks for axial and diagonal propagation.

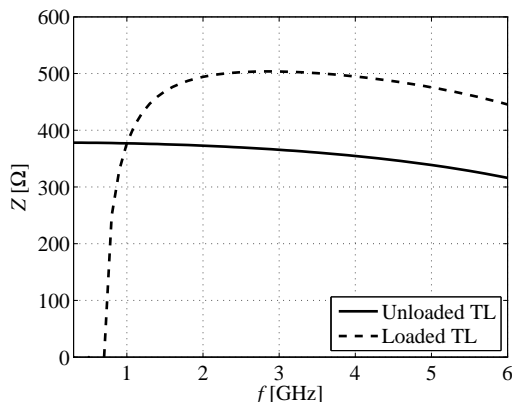


FIG. 3: Impedances of the networks, calculated for axial propagation.

larger bandwidth. The larger bandwidth is expected due to the linear dispersion of the unloaded network. First, we will study the effect of the aforementioned unideal phase velocity on cloaking and then present a simple way of matching the unloaded network with free space.

#### IV. EFFECT OF UNIDEAL PHASE VELOCITY ON CLOAKING

##### A. Scattering from the cloak

To be able to study the effect of unideal phase velocity (which is related only to the unloaded transmission-line cloak), we consider a cloak having ideal impedance-matching with

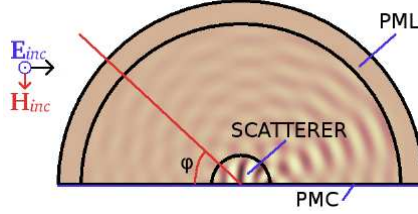


FIG. 4: Model for calculating the scattering cross section of the cloak and reference objects.

the surrounding medium. The transmission-line network is represented as a homogeneous material with certain relative permittivity  $\epsilon_r$  and permeability  $\mu_r$  (with their ratio equal to unity, as in free space). Using (2), it can be found that this homogeneous material should have relative permittivity and permeability equal to  $\sqrt{2}$ . With these parameters the dispersion curve of our homogeneous material lies exactly on the dashed curve of Fig. 2 (i.e., diagonal propagation in the unloaded network). We can conclude that the homogeneous material represents the dispersion of the unloaded network very well for all propagation directions in the region where the network is isotropic (that is, below 3 GHz). In the following, we study a cylinder made of a homogeneous material with  $\epsilon_r = \mu_r = \sqrt{2}$ . The cylinder is infinite in the  $z$ -direction. The diameter of the cylinder is 128 mm. Note that here the period is not defined, for the network is modelled with a homogeneous material.

Scattering cross section [12] is one quantitative measure for the performance of an idealized cloak. Here the scattering cross section is calculated numerically using a Finite Element Method (FEM) based COMSOL Multiphysics software. The simulation setup is the following: the scatterer is placed in the center of a cylinder coated with a perfectly matched layer (PML) and the scatterer (cloak) is illuminated with a plane wave. The geometrical symmetry allows us to cut the problem in half using a perfect magnetic conductor (PMC) boundary, see Fig. 4. From the solved simulation, the scattered field is calculated in all directions around the scatterer. The scattered far field  $E_s$  is calculated from the near field using the Stratton-Chu formula on the inner boundary of the PML [13]. The scattering cross section  $\sigma_s$  is obtained from the scattered far field with

$$\sigma_s(\varphi) = 2\pi R \frac{|E_s|^2}{|E_{inc}|^2}, \quad (6)$$

where  $\varphi$  is the angle,  $R$  is the distance from the center of the scatterer to the inner boundary of the PML, and  $E_{inc}$  is the incident electric field.

The scattering cross section was calculated for the idealized cloak and for an array of vertical rods made of a perfect electric conductor (PEC). The PEC rods have a cross section of  $4 \text{ mm} \times 4 \text{ mm}$  (a realizable cloak period has been assumed to be 8 mm) and the rods are placed in the form of a hexagonally shaped array. The PEC rod array's outer dimensions are smaller than the diameter of the simulated homogenized cloak. The PEC rods constitute the object that could be hidden by the cloak.

The most interesting case to study is the total scattering cross section, where the scattering cross section is integrated over the angle  $\varphi$ . See Fig. 5 for the total scattering of the cloak, calculated from the scattered field obtained from the simulations. Because the cloak is impedance-matched to free space, the back scattering from the (homogeneous) cloak is always below that of the reference object (this was also verified with simulations). From Fig. 5 we can thus conclude that for some frequencies the forward scattering from the cloak is very strong, in some directions even stronger than from the reference object. From Fig. 5 we see that the cloaking efficiency (total scattering from the cloak as compared to the reference case) fluctuates quite strongly, whereas the scattering from the reference object smoothly increases with increasing frequency. We have found that this phenomenon is due to the phase matching at the backside of the cloak. For example, at the frequency 4 GHz, the wave front at the backside of the cloak and in free space are almost in opposite phase. This leads to strong scattering from the backside of the cloak.

On the other hand, as the frequency is increased, the phase difference between the cloak edge and free space becomes smaller and reaches zero at some frequencies. Therefore the cloaking efficiency starts to improve after 4 GHz and around 6 GHz there is a band where the cloak scatters much less than the reference object. Note that good cloaking efficiency is achieved also at low frequencies, where the cloak is small compared to the wavelength, i.e., below 2 GHz in the example case studied here. The scattering from the cloak and from the reference object to different directions, at the frequencies 1 GHz and 6.4 GHz, is plotted in Fig. 6, from which it is obvious that the backscattering from the cloak is strongly reduced and also the forward scattering is considerably lower than that of the reference object (at those specific frequencies). The reader must note that in the scattering simulations the cloak is modelled as a homogeneous material which is fully isotropic at all frequencies. For the studied transmission-line networks (period  $d = 8 \text{ mm}$ ) the isotropy is achieved only below the frequency 3 GHz (approximately), as discussed above. The isotropic region can



be extended to higher frequencies by decreasing the period of the structure, but this has the drawback of reducing the maximum size of the cloaked object's inclusions.

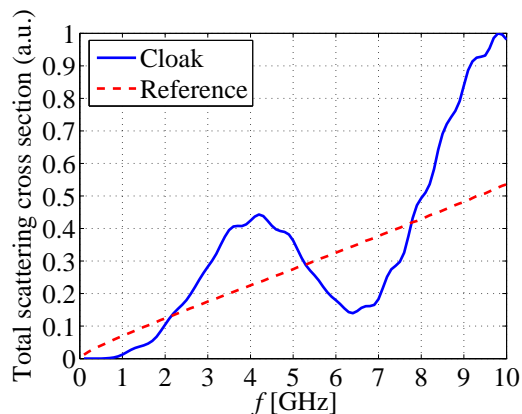
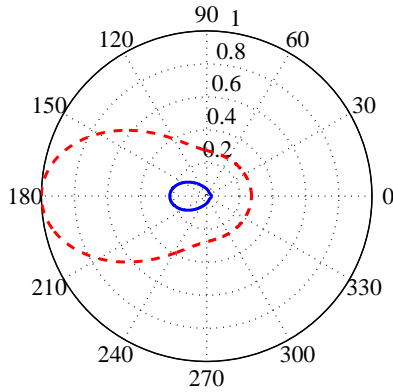


FIG. 5: Simulated total scattering cross section from the cloak and the reference object, normalized to the maximum value of the cloak's total scattering.

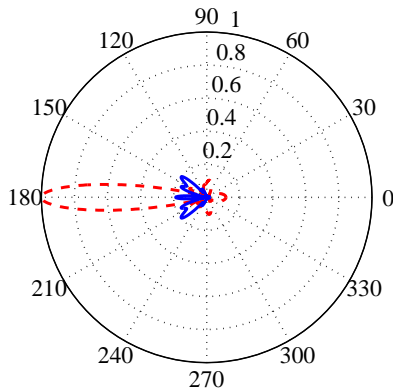
## B. Cloaking from signals

To take advantage of the most promising feature of the cloak proposed in this paper, i.e., cloaking from signals, we have to use the unloaded transmission-line network. This choice has also the advantage of larger operation bandwidth, due to the linear dispersion characteristics and the slowly varying impedance, see Figs. 2 and 3. As discussed above, this choice has the drawback of unideal phase velocity. To obtain more information about the effect of this unideality on cloaking, and especially cloaking from signals, we have simulated the cloak using a Finite-Difference-Time-Domain (FDTD) code. FDTD is suitable for this task, since it inherently includes the possibility of signal excitation.

In the FDTD simulations, we have modeled a cloak having the same diameter as the homogeneous cloak studied above. The diameter of the cylindrical cloak is therefore  $16d = 128$  mm and the period of the interconnecting transmission lines is 8 mm. The cloak has the same dispersion as shown in Fig. 2 (unloaded network). The FDTD code takes into account the anisotropy that occurs at the higher frequencies. To study only the effect of unideal dispersion, we have ideal impedance-matching between the cloak and free space. As a reference object, we again have a mesh of PEC wires, placed in the position of the cloak. The PEC wires form a cylindrically shaped mesh that fits inside the studied cloak. The



(a)



(b)

FIG. 6: Simulated scattered electric field to different directions from the cloak (solid line) and the reference object (dashed line) at the frequencies 1 GHz (a) and 6.4 GHz (b). Both plots are normalized to the maximum value of the reference object scattering. The plane wave that illuminates the cloak/reference object travels in the direction  $\varphi = 180^\circ$

cloak and the reference object are excited by a signal with vertically polarized electric field, i.e.,  $\overline{E}$  is oriented along the  $z$ -axis.

According to Fig. 5, we can expect good cloaking (as compared to the reference object) at frequencies below 2 GHz, and e.g., in the band from 5.5 GHz to 7.5 GHz. See Fig. 7 for the simulation results for pulses with center frequencies at 1 GHz, 2 GHz, and 5.5 GHz. In Fig. 7 snapshots of the electric field distributions are taken at a time step when the signal has just passed the cloak/reference object, i.e., the signal comes from the left and moves to the

right in Fig. 7. The signal bandwidths used in the FDTD simulations are relatively large: in Figs. 7(a),(b) the relative half-power pulse width is 52 % with center frequency  $f_c = 1$  GHz, in Figs. 7(c),(d) it is 26 % with center frequency  $f_c = 2$  GHz and in Figs. 7(e),(f) it is 9.5 % with center frequency  $f_c = 5.5$  GHz.

From Fig. 7 we see that at all the shown frequencies, the backscattering from the cloak is zero, and that inside the cloak, the waves are “delayed,” with respect to the waves propagating in free space (this is due to the shorter wavelength inside the cloak). Because of this, some forward scattering from the cloak occurs, although the shadow generated by the cloak is always well mitigated, as compared to the reference object. The FDTD simulations seem to confirm the cloaking effect, studied for the time-harmonic case in Fig. 5, also for signal excitation. The pulse with center frequency of 5.5 GHz, presented in Figs. 7(e),(f) is already at the frequency range where the network is anisotropic. The transmission-line network in FDTD simulations is not capable of supporting higher frequencies, because the wavelength becomes too short compared to the period of the network. Despite of the anisotropy, Fig. 7(f) demonstrates the benefit of the phase matching inside and outside the cloak: because the

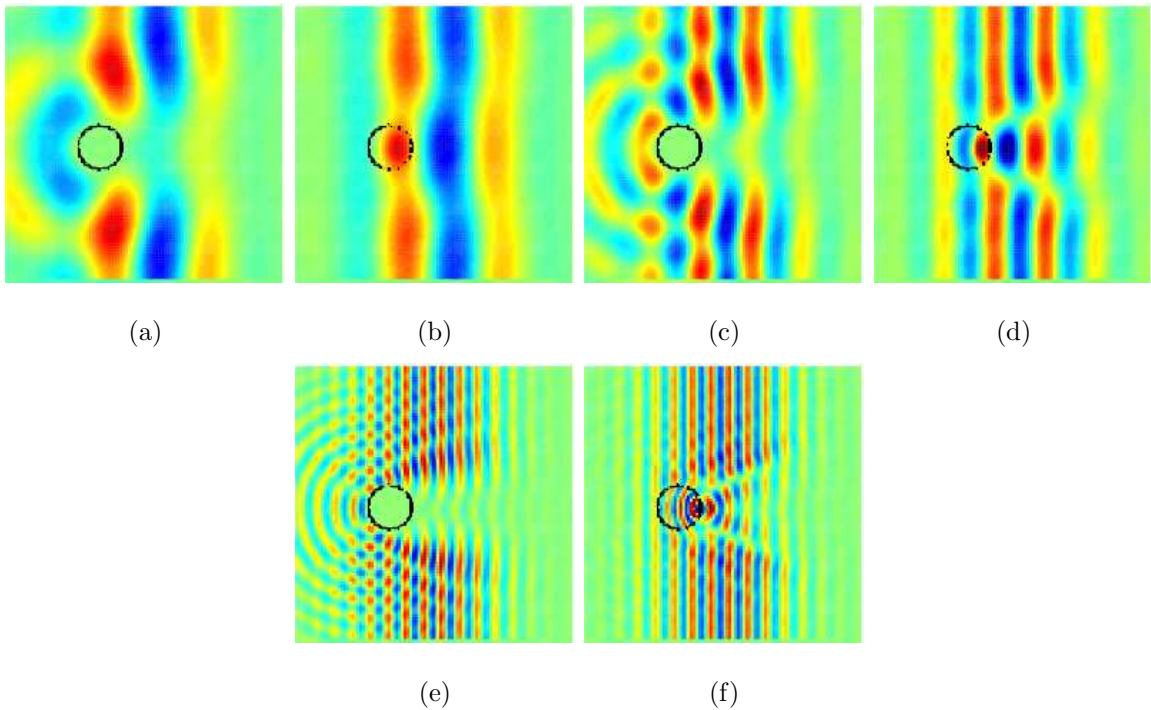


FIG. 7: Color Online. Electric field snapshots from FDTD simulations (all normalized to the same amplitude value). (a) Reference object,  $f_c = 1$  GHz. (b) Cloak,  $f_c = 1$  GHz. (c) Reference object,  $f_c = 2$  GHz. (d) Cloak,  $f_c = 2$  GHz. (e) Reference object,  $f_c = 5.5$  GHz. (f) Cloak,  $f_c = 5.5$  GHz.

waves that emerge from the backside of the cloak are in phase with the waves outside the cloak, the wavefronts at the back of the cloak prevent the formation of a strong shadow.

It is clear that the best cloaking effect (cloak scattering versus the reference object scattering) is always achieved at low frequencies. The phase matching technique can be used if the cloak must be large compared to the wavelength.

## V. SIMULATION OF A REALIZABLE CLOAK

In this section we present a simple way of matching the transmission-line network to free space. Furthermore, we verify the operation of the cloak by numerical full-wave simulations using Ansoft’s High Frequency Structure Simulator (HFSS). The previous sections of this paper were devoted to study of the unideal propagation characteristics of the unloaded network while assuming perfect impedance matching between the cloak and the surrounding medium. In this section we study a transversally infinite slab made of two-dimensional unloaded transmission-line networks, thus effectively studying only the transition from free space to the cloak and vice versa. The reader should notice here that unlike in the previous section, the thickness of the slab does not have any effect on the phase matching between the waves travelling inside and outside of the cloak for the cloak is infinite in the transversal direction. However, since the wavelength inside the slab differs from that in free space we expect to see Fabry-Perot type resonances in the reflection and transmission coefficients due to the finite electrical length of the slab (along the  $x$ -axis).

The periodical boundary conditions allow us to simplify the simulation model: We need to model only one “unit cell” of the infinite slab as shown in Fig. 8. The slab shown in Fig. 8 is infinite in the  $y$ - and  $z$ -directions, but along the  $x$ -axis it is finite with thickness of  $16d = 128$  mm.

Based on the simulated scattering and the FDTD results, we have decided to tune the network impedance in order to obtain the impedance matching at higher frequencies (around 6 GHz). Effectively this means that the impedance of single sections of transmission lines should be increased to raise the curve shown in Fig. 3 to obtain the impedance of  $377 \Omega$  at a frequency near 6 GHz. Using the impedance equations from [9] we have found that the transmission-line impedance of  $600 \Omega$  results in the network impedance of  $377 \Omega$  at approximately 5.2 GHz. As the transmission lines, we have chosen to use parallel metal strips due

to the large range of impedance values available and the simple geometry and easy manufacturing of this type of transmission line. Using the simple parallel-plate approximation, we have calculated the width  $w$  and height  $h$  of the transmission line to be 1.257 mm and 2 mm, respectively. The metal strips are modelled as infinitely thin and perfectly conducting to reduce the simulation time.

Matched transition from free space to the cloak and vice versa can be obtained by extending the transmission lines at the both sides of the cloak, while preserving the impedance of the transmission lines. This way the both slab surfaces are covered with small sections of transmission lines, effectively operating as antennas with their input impedance equal to the free space impedance. See Fig. 9 for the HFSS simulation model of the “unit cell” of the slab.

As shown in Fig. 9, the antennas cover almost all of the area of the unit cell in the  $yz$ -plane, but in fact, there is a tiny gap left between the antennas of the neighboring unit cells (approximately  $2 \mu\text{m}$  in the  $z$ -direction and  $120 \mu\text{m}$  in the  $y$ -direction). The width and height of the simulated unit cell are 8 mm and 12.73 mm, respectively, to preserve the correct impedance of the transmission lines ( $12.73/8 \approx 2/1.257$ ). We have also placed a reference object that we want to cloak, inside the network, see Fig. 9. This reference object is an array of rods made of PEC, as in the scattering simulations. The rods have a cross-section of  $4 \text{ mm} \times 4 \text{ mm}$  and they are effectively infinite along the  $z$ -axis.

The cloak is excited with a plane wave having the electric field parallel to the  $z$ -axis. First, we have studied the case of the normal incidence angle (magnetic field  $\vec{H}$  is parallel to

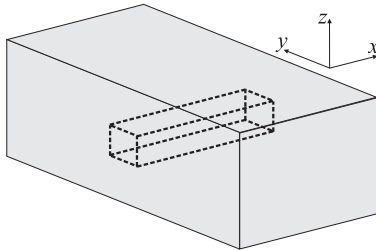


FIG. 8: The modeled slab made of two-dimensional transmission-line networks which are placed on top of each other. The slab is infinite in the  $y$ - and  $z$ -directions. The dashed line shows a single “unit cell” of the slab, which can be easily modelled with full-wave simulators using periodic boundaries.

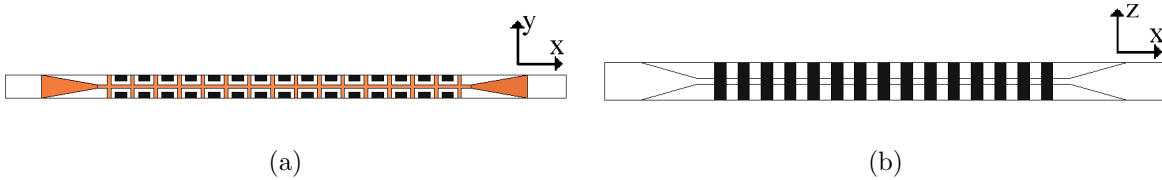


FIG. 9: HFSS model of the cloak with reference object inside (a) viewed from the top and (b) viewed from the side. The reference object is illustrated with black color.

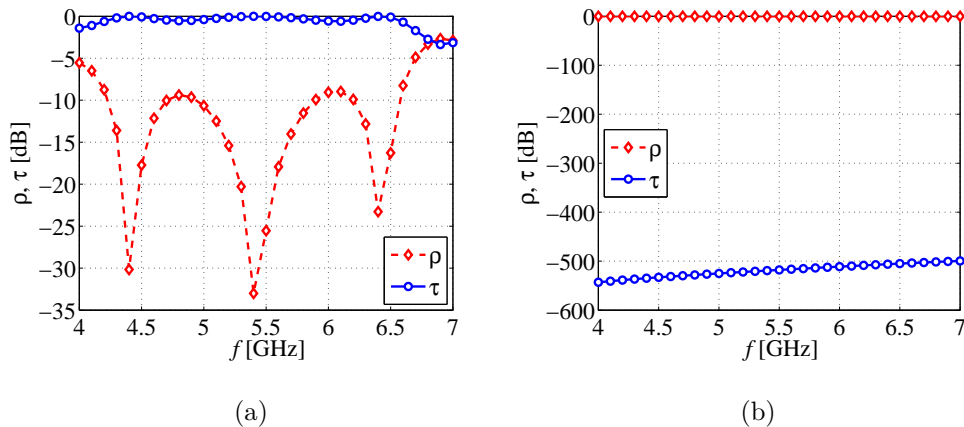


FIG. 10: Simulated reflection and transmission for (a) cloak slab with reference object inside and (b) reference object. A plane wave illuminates the cloak slab with normal incidence angle.

the  $y$ -axis). See Fig. 10(a) for the simulated reflection ( $\rho$ ) and transmission ( $\tau$ ) coefficients for the cloak with the reference object inside and Fig. 10(b) for  $\rho$  and  $\tau$  in the case of the reference object only.

From Fig. 10 it is obvious that the reference object behaves effectively as a solid metal slab reflecting basically all of the incident field, whereas the same object placed inside the cloak is almost transparent to the incident field. We believe that the resonances seen in the reflection and transmission through the cloak are due to the finite thickness of the cloak, as discussed above. The minimum of the envelope of the reflection coefficient in Fig. 10(a) occurs at approximately 5.4 GHz, which is close to the expected value of 5.2 GHz, which was obtained from the analytical expressions for the network impedance.

The effect of oblique incidence angle was also considered for two cases:  $\phi = 30^\circ$  and  $\phi = 60^\circ$ , where  $\phi$  is the angle in the  $xy$ -plane, i.e., the electric field  $\vec{E}$  is always directed along the  $z$ -axis. See Fig. 11 for the simulation results of the reflection coefficient  $\rho$  as a function of the frequency for these two incidence angles.

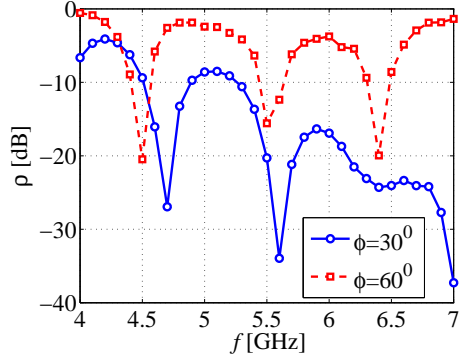


FIG. 11: Simulated reflection coefficients for the cloak with reference object inside. Oblique incidence angles of  $\phi = 30^\circ$  and  $\phi = 60^\circ$  are considered.

Note that the positions of the resonance frequencies seen in the reflection coefficient are affected by the oblique incidence due to the shift in the Fabry-Perot resonances: the effective thickness of the slab changes as the incidence angle changes. At frequencies above 3 GHz the transmission-line networks studied in this paper are anisotropic, which also changes the electrical thickness of the slab for different incidence angles. Nevertheless, for the frequencies 5.5 GHz and 6.4 GHz, the reflection coefficient remains very low for all the studied incidence angles.

## VI. CONCLUSIONS

We have shown that transmission lines can be used to cloak objects from electromagnetic fields. The object or objects that can be cloaked have to be smaller than the period of the cloak itself, which is composed of either loaded or unloaded transmission-line networks. The propagation characteristics of the transmission-line network have to mimic the propagation in the medium that surrounds the cloak. If this medium is free space, the optimal propagation characteristics of the cloak cannot be achieved with an unloaded network. A periodically loaded transmission-line network on the other hand can be designed to have ideal propagation characteristics, but the operation of this cloak is very narrowband and it suffers from similar unidealities as the cloak designs presented in the literature. The unloaded transmission-line networks seem to be more prospective for applications that require simple manufacturing and large bandwidth.

We have thoroughly studied the effect of unideal propagation characteristics on the cloak-

ing effect and have shown that when the cloak is small enough as compared to the wavelength, good cloaking efficiencies are achieved. Also, at higher frequencies the cloaking effect is achieved at frequencies that depend on the physical size of the cloak. This is due to the phase matching of the wave at the backside of the cloak and the wave in the surrounding medium. We have shown how a realizable transmission-line network can be matched to free space and have presented full-wave simulations for a slab made of such a network placed in free space.

### Acknowledgements

This work was initially started as a student project work at the TKK Radio Laboratory and the TKK Electromagnetics Laboratory within a postgraduate course “Metamaterials in Electromagnetics and Radio Engineering.” The authors wish to thank Mr. A. Karttunen, Mr. G. Molera, Mr. H. Rimminen, Mr. M. Vaaja and Prof. A. Sihvola for useful discussions during that course.

This work has been partially funded by the Academy of Finland and TEKES through the Center-of-Excellence program. Pekka Alitalo wishes to thank the Graduate School in Electronics, Telecommunications and Automation (GETA) and the Nokia Foundation for financial support. Liisi Jylhä would like to thank GETA for financial support.

- 
- [1] U. Leonhardt, Optical conformal mapping, *Science*, Vol. 312, pp. 1777–1780, 2006.
  - [2] J.B. Pendry, D. Schurig, and D.R. Smith, Controlling electromagnetic fields, *Science*, Vol. 312, pp. 1780–1782, 2006.
  - [3] A. Alù and N. Engheta, Plasmonic materials in transparency and cloaking problems: mechanism, robustness, and physical insights, *Optics Express*, Vol. 15, No. 6, pp. 3318–3332, 2007.
  - [4] W. Cai, U. K. Chettiar, A. V. Kildishev, and V. M. Shalaev, Optical cloaking with non-magnetic metamaterials, *Nature Photonics*, Vol. 1, pp. 224–227, 2007; published online.
  - [5] D. Schurig, J.J. Mock, B. J. Justice, S.A. Cummer, J.B. Pendry, A.F. Starr, and D.R. Smith, Metamaterial electromagnetic cloak at microwave frequencies, *Science*, Vol. 314, pp. 977–980, 2006.



- [6] P.-S. Kildal, A. A. Kishk, and A. Tengs, Reduction of forward scattering from cylindrical objects using hard surfaces, *IEEE Trans. Antennas Propag.*, Vol. 44, No. 11, pp. 1509–1520, 1996.
- [7] C. Caloz, H. Okabe, T. Iwai, and T. Itoh, “Transmission line approach of left-handed (LH) materials,” in *Proc. USNC/URSI National Radio Science Meeting*, vol. 1, San Antonio, TX, June 2002, p. 39.
- [8] G. V. Eleftheriades, A. K. Iyer, and P. C. Kremer, “Planar negative refractive index media using periodically  $L$ - $C$  loaded transmission lines,” *IEEE Trans. Microwave Theory Tech.*, vol. 50, no. 12, pp. 2702–2712, Dec. 2002.
- [9] P. Alitalo, S. Maslovski, and S. Tretyakov, Three-dimensional isotropic perfect lens based on LC-loaded transmission lines, *Journal of Applied Physics*, Vol. 99, 064912, 2006.
- [10] A. Grbic and G. V. Eleftheriades, “An isotropic three-dimensional negative-refractive-index transmission-line metamaterial,” *J. Appl. Phys.*, vol. 98, p. 043106, 2005.
- [11] W. J. R. Hoefler, P. P. M. So, D. Thompson, and M. M. Tentzeris, “Topology and design of wide-band 3D metamaterials made of periodically loaded transmission line arrays,” *2005 IEEE MTT-S International Microwave Symposium Digest*, pp. 313–316, June 2005.
- [12] A. F. Peterson, S. L. Ray, R. Mittra, *Computational Methods for Electromagnetics*, IEEE Press, New York, 1998.
- [13] Y. T. Lo, S. W. Lee, *Antenna Handbook, Theory, Applications and Design*, Van Nostrand Reinhold Company, New York, 1988.